Acta Crystallographica Section D
Biological Crystallography
ISSN 0907-4449

Structure of grouper iridovirus purine nucleoside phosphorylase

You-Na Kang,[a] Yang Zhang,[a] Paula W. Allan,[b] William B. Parker,[b] Jing-Wen Ting,[c] Chi-Yao Chang[c] and Steven E. Ealick[a]*

[a]Department of Chemistry and Chemical Biology, Cornell University, Ithaca, NY 14853-1301, USA, [b]Southern Research Institute, Birmingham, AL 35205, USA, and [c]The Institute of Cellular and Organismic Biology, Academia Sinica, Taipei 115, Taiwan

Correspondence e-mail: see3@cornell.edu

Received 6 October 2009
Accepted 13 November 2009

PDB Reference: grouper iridovirus PNP, 3khs.

Purine nucleoside phosphorylase (PNP) catalyzes the reversible phosphorolysis of purine ribonucleosides to the corresponding free bases and ribose 1-phosphate. The crystal structure of grouper iridovirus PNP (givPNP), corresponding to the first PNP gene to be found in a virus, was determined at 2.4 Å resolution. The crystals belonged to space group $R3$, with unit-cell parameters $a = 193.0$, $c = 105.6$ Å, and contained four protomers per asymmetric unit. The overall structure of givPNP shows high similarity to mammalian PNPs, having an α/β structure with a nine-stranded mixed β-barrel flanked by a total of nine α-helices. The predicted phosphate-binding and ribose-binding sites are occupied by a phosphate ion and a Tris molecule, respectively. The geometrical arrangement and hydrogen-bonding patterns of the phosphate-binding site are similar to those found in the human and bovine PNP structures. The enzymatic activity assay of givPNP on various substrates revealed that givPNP can only accept 6-oxopurine nucleosides as substrates, which is also suggested by its amino-acid composition and active-site architecture. All these results suggest that givPNP is a homologue of mammalian PNPs in terms of amino-acid sequence, molecular mass, substrate specificity and overall structure, as well as in the composition of the active site.

1. Introduction

Purine nucleoside phosphorylase (PNP; EC 2.4.2.1) is a ubiquitous enzyme that catalyzes the reversible phosphorolysis of purine ribonucleosides to the corresponding free bases and ribose 1-phosphate with inversion of the configuration of ribose 1-phosphate from β to α. PNP plays a key role in the purine-salvage pathway, which allows cells to reutilize purine bases for the synthesis of purine nucleotides (Montgomery, 1993; Parks & Agarwal, 1973; Stoeckler, 1984). Based on molecular mass, protein structure and substrate specificity, PNPs can be classified into two classes: trimeric PNPs and hexameric PNPs. Trimeric PNPs are composed of three identical protomers, each with a mass of about 31 kDa. They are mainly found in mammals but are also found in some microorganisms. On the other hand, hexameric PNPs are composed of six identical protomers, each with a mass of about 26 kDa, and only occur in microorganisms. Interestingly, some microorganisms, including *Escherichia coli* and several *Bacillus* species, possess both classes of PNP (Hammer-Jespersen *et al.*, 1980; Senesi *et al.*, 1976; Jensen, 1978). Whereas trimeric PNPs are only active on 6-oxopurine nucleosides, hexameric PNPs

generally accept both 6-oxo and 6-aminopurine nucleosides as substrates (Bzowska *et al.*, 1990, 2000); however, there are a few exceptions. For instance, hexameric PNP from *Plasmodium falciparum* does not cleave adenosine (Daddona *et al.*, 1986), while hexameric *B. cereus* PNP is specific for adenosine (Sgarrella *et al.*, 2007). Although the two classes of PNP do not share significant sequence similarity, they are structurally similar, having a protomeric fold consisting of a distorted β-barrel flanked by α-helices on each side. Differences in the active-site composition of the two classes result in their different substrate specificity (Bzowska *et al.*, 2000; Mao *et al.*, 1997).

Iridoviruses are large icosahedral cytoplasmic deoxyriboviruses that contain a circularly permutated and terminally redundant double-stranded DNA genome ranging from 103 to 212 kbp in length (Jakob *et al.*, 2001; Schnitzler *et al.*, 1987). Grouper iridovirus (giv), isolated from the spleen tissue of yellow grouper (*Epinephelus awoara*), is a causative agent of an epizootic fish disease and this infection is a serious problem in modern aquaculture and fish farming (Lai *et al.*, 2000). Recently, a complete genome-sequence analysis of grouper iridovirus revealed the presence of a gene encoding PNP (givPNP) which has not been found in other iridoviruses or in any other viruses (Lai *et al.*, 2000; Ting *et al.*, 2004; Tsai *et al.*, 2005). givPNP is composed of 285 amino-acid residues with a molecular mass of approximately 30 kDa and is localized in the cytoplasm of giv-infected host cells. The amino-acid sequence of givPNP is 48.1, 46.7 and 45.3% identical to those of human, bovine and mouse PNPs, respectively, with the active-site residues being highly conserved (Fig. 1). Phylogenetic analysis indicates that givPNP is evolutionarily closely related to mammalian PNPs (Ting *et al.*, 2004).

Here, we report the crystal structure of givPNP, the first viral PNP to be identified, at 2.4 Å resolution. givPNP is structurally homologous to other mammalian PNPs, with a similar protomeric fold and trimeric arrangement. A phosphate ion and a Tris molecule from the crystallization solution were bound at the predicted phosphate-binding and ribose-binding sites, respectively. Although the preliminary HPLC analysis suggested that givPNP can accept not only guanosine and inosine but also adenosine as a substrate (Ting *et al.*, 2004), enzymatic activity assay data on the highly purified enzyme showed that like mammalian PNPs givPNP can only cleave 6-oxopurine nucleosides.

2. Materials and methods

2.1. Protein expression and purification

Recombinant givPNP was expressed in *Escherichia coli* as described previously (Ting *et al.*, 2004). The expression vector pET-20b(+) containing givPNP was transformed into B834pLysS competent cells. Cells were grown in LB medium containing ampicillin (0.1 mg ml^{-1}) at 309 K with shaking. When an OD_{600} of 0.6 was reached, isopropyl β-D-1-thiogalactopyranoside was added to a final concentration of

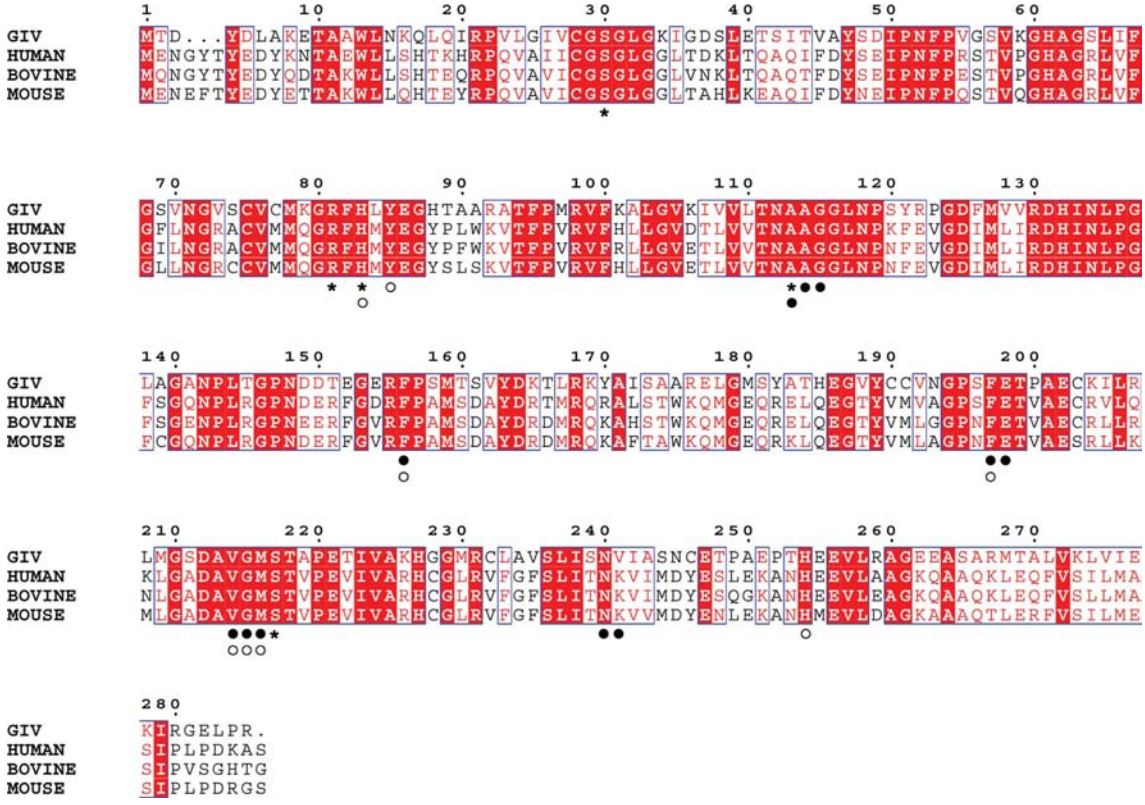

Figure 1
Multiple amino-acid sequence alignment of givPNP with other mammalian PNPs (GIV, Q5YBA4; human, P00491; bovine, P55859; mouse, P23492). All residues involved in the phosphate-binding (asterisks), ribose-binding (circles) and purine base-binding (filled circles) sites are highly conserved.

Table 1
Data-collection statistics for the givPNP structure.

Values in parentheses are for the highest resolution shell.

X-ray source	Cu $K\alpha$
Space group	$R3$
Unit-cell parameters (Å)	a = 193.0, c = 105.6
Resolution range (Å)	50.0–2.38 (2.47–2.38)
Measured reflections	186181 (18508)
Unique reflections	58889 (5946)
Redundancy	3.2 (3.1)
$I/\sigma(I)$	24.8 (3.1)
Completeness (%)	100 (99.9)
$R_{\rm merge}$† (%)	5.2 (40.4)

† $R_{\rm merge} = \sum_{hkl}\sum_i |I_i(hkl) - \langle I(hkl)\rangle|/\sum_{hkl}\sum_i I_i(hkl)$, where $\langle I(hkl)\rangle$ is the mean intensity of the i reflections with intensities $I_i(hkl)$ and common indices hkl.

0.2 m*M* for induction and the cells were incubated at 302 K with shaking for 3–4 h before harvesting by centrifugation. The cell pellet was resuspended in equilibration/wash buffer (50 m*M* sodium phosphate buffer pH 7.0 containing 300 m*M* NaCl) and lysed by sonication. After removing the cell debris by centrifugation, the supernatant was collected and applied onto a BD TALON cobalt metal-affinity column (Qiagen) previously equilibrated with equilibration/wash buffer. The bound protein was eluted with elution buffer (150 m*M* imidazole in equilibration/wash buffer). The purified recombinant protein was buffer-exchanged into 20 m*M* Tris–HCl pH 7.5 by dialysis and concentrated to about 12.5 mg ml^{-1} using Amicon Ultra 15 (10 kDa molecular-weight cutoff; Millipore) and stored at 192 K for subsequent use. SDS–PAGE analysis showed that the givPNP was more than 99% pure (data not shown).

2.2. Crystallization

Purified givPNP was crystallized using the hanging-drop vapor-diffusion method. Crystals were grown in 15–17%(*w*/*v*) PEG 1000 and 0.1 *M* Tris–HCl pH 8.0. Drops were prepared by mixing 2 µl protein solution (12.5 mg ml^{-1}) with 2 µl reservoir solution. The drops were placed on siliconized cover slips and equilibrated against 0.5 ml reservoir solution at a temperature of 295 K. Crystals appeared after 2–3 weeks with dimensions of 0.4 × 0.4 × 0.2 mm. The crystals belonged to space group $R3$, with unit-cell parameters a = 193.0, c = 105.6 Å. The Matthews coefficient ($V_{\rm M}$ = 3.12 Å^3 Da^{-1}; Matthews, 1968) suggested the presence of four protomers per asymmetric unit, with a solvent content of 61%.

2.3. Data collection and processing

Prior to data collection, givPNP crystals were cryoprotected using a solution containing the mother liquor with a slightly higher concentration of PEG 1000 and 20% glycerol before freezing them directly in a nitrogen-gas stream at 100 K. The X-ray diffraction data for givPNP were collected on an R-AXIS IV^{++} image-plate detector using Cu $K\alpha$ radiation from a rotating-anode generator. Data were collected by the standard oscillation method in 0.5° increments with an exposure time of 240 s per image and a crystal-to-detector distance of 150 mm. Diffraction data were processed using the *HKL*-2000 program package (Otwinowski & Minor, 1997). Data-collection statistics are summarized in Table 1.

Table 2
Refinement statistics for the givPNP structure.

Values in parentheses are for the highest resolution shell.

Resolution range (Å)	10–2.38 (2.47–2.38)
Total No. of non-H atoms	
No. of protein atoms	7897
No. of ligand atoms	52
No. of water atoms	194
Reflections used	56658 (5346)
Completeness (%)	96.2 (90.6)
R factor† (%)	21.4
$R_{\rm free}$‡ (%)	25.5
Average B factor (Å^2)	47.7
R.m.s.d.s from ideal geometry	
Bond lengths (Å)	0.01
Bond angles (°)	1.60
Ramachandran plot (%)	
Most favored	91.1
Additionally allowed	8.2
Generously allowed	0.3
Disallowed	0.5

† R factor = $\sum_{hkl}||F_{\rm obs}| - |F_{\rm calc}||/\sum_{hkl}|F_{\rm obs}|$, where $F_{\rm obs}$ and $F_{\rm calc}$ are the observed and calculated structure factors, respectively. ‡ For $R_{\rm free}$ the sum extends over a subset of reflections (10%) excluded from all stages of refinement.

2.4. Structure determination, model building and refinement

The crystal structure of givPNP was determined by molecular replacement using the human PNP trimer (PDB code 1ula; Ealick *et al.*, 1990) as a search model with the program *Crystallography & NMR System* (*CNS*; Brünger *et al.*, 1998). The structure was refined by multiple cycles of simulated-annealing, energy-minimization and temperature-factor refinement using *CNS* and manual rebuilding using the programs *O* (Jones *et al.*, 1991) and *Coot* (Emsley & Cowtan, 2004). A total of 10% of the reflections, which were randomly chosen and excluded from the refinement, were used for the calculation of $R_{\rm free}$. Tight noncrystallographic symmetry (NCS) restraints were applied during the initial rounds of refinement and were gradually released in later rounds. Water molecules were picked automatically using *CNS* (Brünger *et al.*, 1998) and were inspected individually using *O* (Jones *et al.*, 1991) and *Coot* (Emsley & Cowtan, 2004).

2.5. Figure preparation and PDB deposition

Figures were created using *PyMOL* (DeLano, 2002), *MolScript* (Kraulis, 1991) or *BobScript* (Esnouf, 1997) and *Raster3D* (Merritt & Bacon, 1997). The multiple sequence alignment was performed with *ClustalX* (Thompson *et al.*, 1997) and *ESPript* (Gouet *et al.*, 1999). Atomic coordinates and structure factors for givPNP have been deposited in the PDB as entry 3khs.

2.6. givPNP activity assay

givPNP was incubated with various nucleosides in 1 ml solution containing 50 m*M* potassium phosphate pH 7.4, 100 µ*M* substrate and an appropriate amount of enzyme so that a linear increase in product formation could be followed

over time. After incubation for 0, 0.25, 0.5, 1 and 2 h at 297 K, 150 µl of the solution was removed and mixed with 150 µl water and the reaction was stopped by boiling. The precipitated proteins were removed by filtration (0.2 µm syringe filter) and the sample was injected onto a 5 µm BDS Hypersil C-18 column (150 × 4.6 mm; Keystone Scientific Inc., State College, Pennsylvania, USA). The mobile phase was an isocratic elution at a flow rate of 1 ml min^{-1} using 50 m*M* ammonium dihydrogen phosphate buffer pH 4.5 containing either 1% acetonitrile for inosine, deoxyinosine, guanosine or deoxyguanosine, or 2.5% acetonitrile for adenosine. The nucleosides and their respective bases were detected as they eluted from the column by their absorbance at 254 nm. Each reported value (Table 3) represents the mean of at least two determinations.

3. Results and discussion

3.1. Quality of the final model

The givPNP structure contained four protomers in the asymmetric unit (designated *A*, *B*, *C* and *D*), with protomers *A*, *B* and *C* forming a complete trimer while protomer *D* is one third of a trimer generated by the crystallographic symmetry.

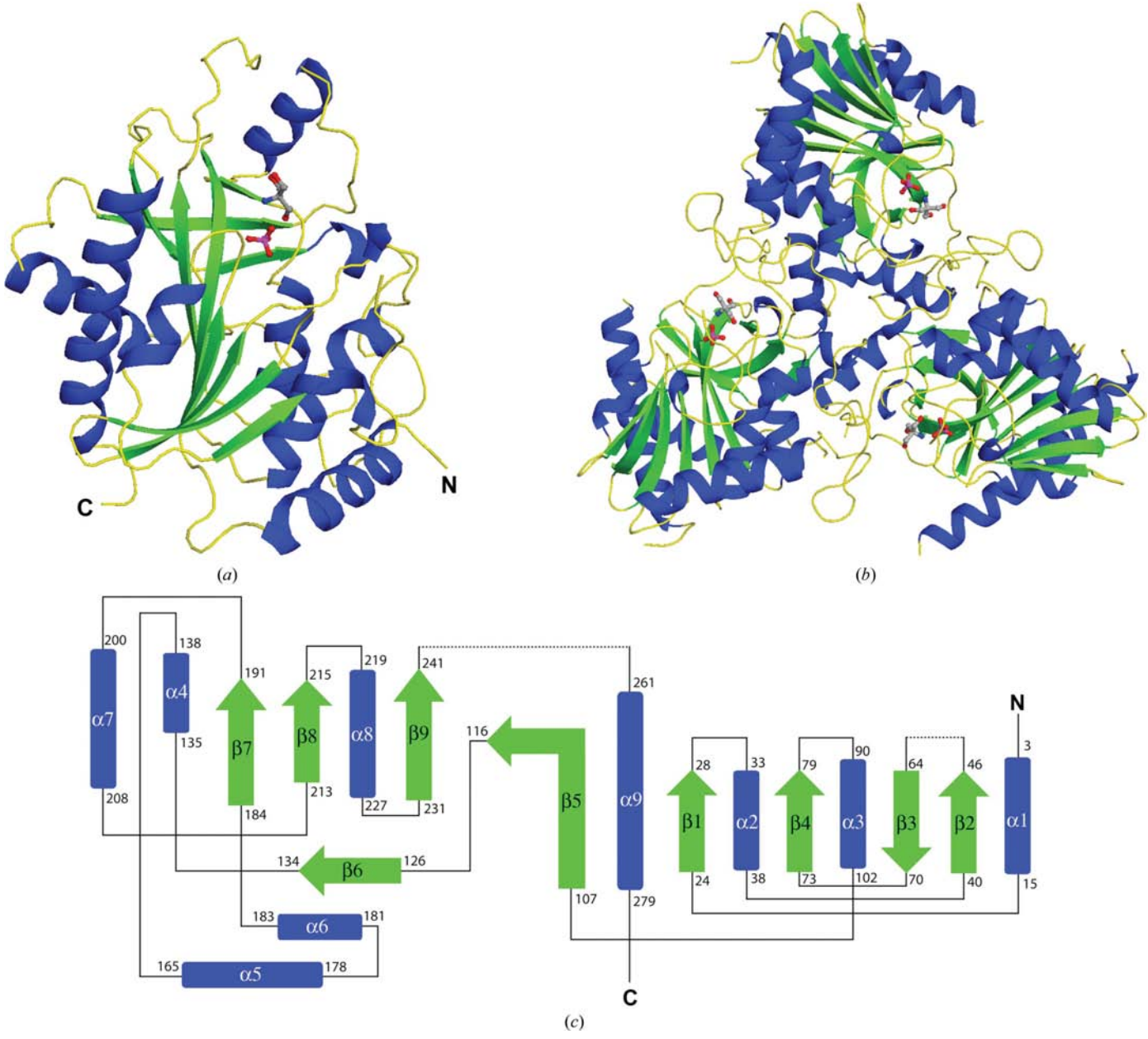

Figure 2
Overall structure of givPNP. (*a*) A ribbon diagram of the protomer of givPNP. β-Strands are colored green and α-helices are colored blue. The phosphate ion and Tris molecule are represented as ball-and-stick models (magenta, phosphate; grey, carbon; blue, nitrogen; red, oxygen). (*b*) Trimer of givPNP with the view down the threefold axis. (*c*) Topology diagram of givPNP. The dashed line indicates a disordered region of the structure.

The root-mean-square deviations (r.m.s.d.s) between the four protomers in the asymmetric unit were 0.08–0.1 Å. In the final model chain *A* contained residues 1–54, 62–247 and 260–283, chain *B* contained residues 1–56, 62–247 and 256–283, chain *C* contained residues 1–57, 62–248 and 260–285, and chain *D* contained residues 1–55, 63–247 and 260–281. The missing residues belonged to two flexible loops: the loop connecting β2 and β3 and the loop between β9 and α9. A phosphate ion and a Tris molecule were found in the active site of each protomer. There were a total of 195 water molecules in the structure. The final R and $R_{\rm free}$ factors of the model were 21.4% and 25.5%, respectively. The model was assessed with *PROCHECK* (Laskowski *et al.*, 1993) and the Ramachandran plot (Ramachandran *et al.*, 1963) showed that 91.1% of the main-chain dihedral angles lay in the most favorable region and 8.2% lay in the additional favored region. One residue, Thr218, in each protomer was in the disallowed region of the Ramachandran plot; however, the electron density was clear. The carbonyl group of Thr218 accepts a hydrogen bond from the main-chain amide of Thr222 as part of the helical hydrogen-bond network for α8 (residues 219–227), while its main-chain amide donates a hydrogen bond to the side chain of Glu221. The unusual resultant geometry may possibly be important for the proper folding of α8. A proline residue (Pro195) near the active site forms a *cis*-peptide bond. The refinement statistics are shown in Table 2.

3.2. Overall structure of givPNP

The overall structure of givPNP is similar to the structures of human PNP (Ealick *et al.*, 1990; Narayana *et al.*, 1997) and bovine PNP (Mao *et al.*, 1998). The biologically active form of givPNP is a homotrimer with a triangular shape, with approximate dimensions of 70 × 70 × 40 Å (Fig. 2*b*). The core of the givPNP protomer has an α/β structure with a nine-stranded mixed β-barrel surrounded by four α-helices on one side and five on the other (Figs. 2*a* and 2*c*). The active sites, which are located at the trimer interface and formed by residues from two adjacent protomers, are occupied by a phosphate ion and a Tris molecule. Interestingly, givPNP contains a total of eight cysteine residues (Cys28, Cys75, Cys77, Cys190, Cys191, Cys203, Cys232 and Cys246), whereas other mammalian PNPs contain only three or four cysteine residues. One of the conserved cysteines, Cys28, is located near the active site. Chemical modification of this cysteine residue in the human enzyme (Cys31 in human PNP) affects the enzymatic activity by blocking substrate entry (Erion, Stoeckler *et al.*, 1997). A disulfide bond which is not observed in mammalian PNPs is formed between residues Cys203 and Cys246 in each givPNP protomer and is represented by good electron density.

3.3. Phosphate-binding site

The givPNP crystal structure contains a phosphate ion in each protomer, which was probably acquired from the purification buffers (Fig. 3). The phosphate-binding site of givPNP is similar to those of mammalian PNP structures (Ealick *et al.*, 1990; Mao *et al.*, 1998), consisting of Ser30, Arg81, His83, Ala113, Ser217 and a water molecule, forming a total of nine hydrogen bonds (Fig. 3*b*). All of the amino-acid residues that are involved in phosphate binding are strictly conserved in all mammalian PNPs (Fig. 1).

3.4. Ribose-binding site occupied by a Tris molecule

In the present structure, a Tris molecule was found near the predicted ribose-binding site (Fig. 3), which is located adjacent to the phosphate-binding site. The crystallization buffer contained Tris and the active-site Tris molecule is presumably derived from the crystallization solution. In the structure of givPNP, the N and O1 atoms of Tris make hydrogen bonds to the O4 atom of the phosphate ion and the main-chain N atom

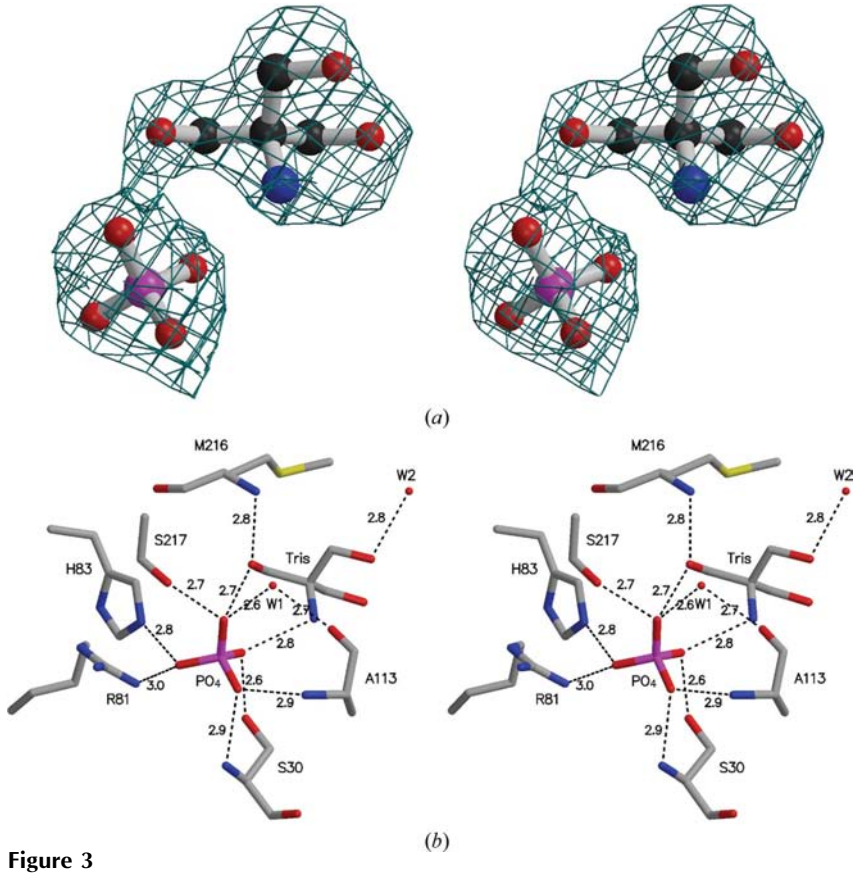

Figure 3
Stereoview of the active site. (*a*) The phosphate ion and Tris molecule are shown in ball-and-stick representation with the same color codes as in Fig. 2. The electron-density map is a simulated-annealing OMIT map contoured at 1σ and is shown in dark cyan. (*b*) Stereoview of the phosphate-binding site of givPNP. Water molecules are shown as red spheres. Hydrogen bonds are represented as dashed lines.

Table 3
Enzymatic activity of givPNP for various substrates.

Substrate	*N*	Activity (nmol mg^{-1} h^{-1})
Inosine	4	208 000 ± 135 000
2′-Deoxyinosine	2	57 000 ± 5000
Guanosine	3	132 000 ± 42 000
2′-Deoxyguanosine	2	70 000 ± 21 000
Adenosine	3	45†

† No activity was detected in two of the experiments at 1 µg ml^{-1}, but when the protein concentration was increased to 10 µg ml^{-1} activity was detected with adenosine at a rate of 45 nmol mg^{-1} h^{-1}.

of Met216, respectively. One water molecule (W2) is at a hydrogen-bonding distance from the Tris O2 atom (Fig. 3*b*). The aromatic ring of Phe156′ from the adjacent subunit is about 3.8–4 Å away from the C3 atom of Tris and makes van der Waals contacts. A Tris molecule with a similar geometry was also reported in the ribose-binding site of hyperthermophilic *Sulfolobus solfataricus* 5′-deoxy-5′-methylthioadenosine phosphorylase (SsMTAP), which is a member of the hexameric PNP family and functions to recycle methylthioadenosine generated during polyamine biosynthesis (Appleby *et al.*, 2001). In the SsMTAP structure, a Tris molecule was only observed in combination with phosphate binding and it was hydrogen bonded to the phosphate ion as well as to the amino acids that normally participate in ribose binding.

3.5. Enzymatic assay of givPNP

The previous HPLC analysis suggested that givPNP is active on guanosine, inosine and adenosine, with metabolic activities of 31.2, 6.7 and 21.2%, respectively (Ting *et al.*, 2004). However, these experiments only detected the disappearance of the substrates and not the appearance of the products. The enzymatic assay in this study revealed that givPNP has high activity on the 6-oxopurine nucleosides inosine, 2′-deoxyinosine, guanosine and 2′-deoxyguanosine. Almost no activity was detected with adenosine, indicating that 6-aminopurines are not good substrates for givPNP (Table 3). These results demonstrate that givPNP has the same substrate specificity as mammalian PNPs, only accepting 6-oxopurine nucleosides as substrates.

3.6. Comparison of the givPNP with mammalian PNPs

The overall structure of givPNP is very similar to those of human (PDB codes 1ula and 1ulb; Ealick *et al.*, 1990) and bovine PNPs (PDB codes 1a9o and 1a9s; Mao *et al.*, 1998) (Fig. 4*a*). Other than the regions involved in crystal-packing contacts, the most significant differences between givPNP and mammalian PNPs are in a flexible loop region (residues 241–260). This region is the most mobile region in all trimeric PNP structures and undergoes a ligand-dependent conformational change, acting as an active-site flap (Fig. 4*a*). The role of this active-site flap in human and bovine PNPs is to serve as a gate that shields the active site from solvent and allows the entrance of the substrates and the release of the products (Ealick *et al.*, 1991; Mao *et al.*, 1998). In givPNP the disulfide bond between Cys203 and Cys246 is located at the starting point of this flexible loop. The rigid disulfide bond alters the first part of this loop, resulting in a conformation that differs from those of mammalian PNPs. However, it is unclear whether the formation of the disulfide bond is physiologically relevant or whether it is an artifact of protein purification and crystallization.

Fig. 4(*b*) shows an active-site superposition of givPNP–PO_4–Tris with the

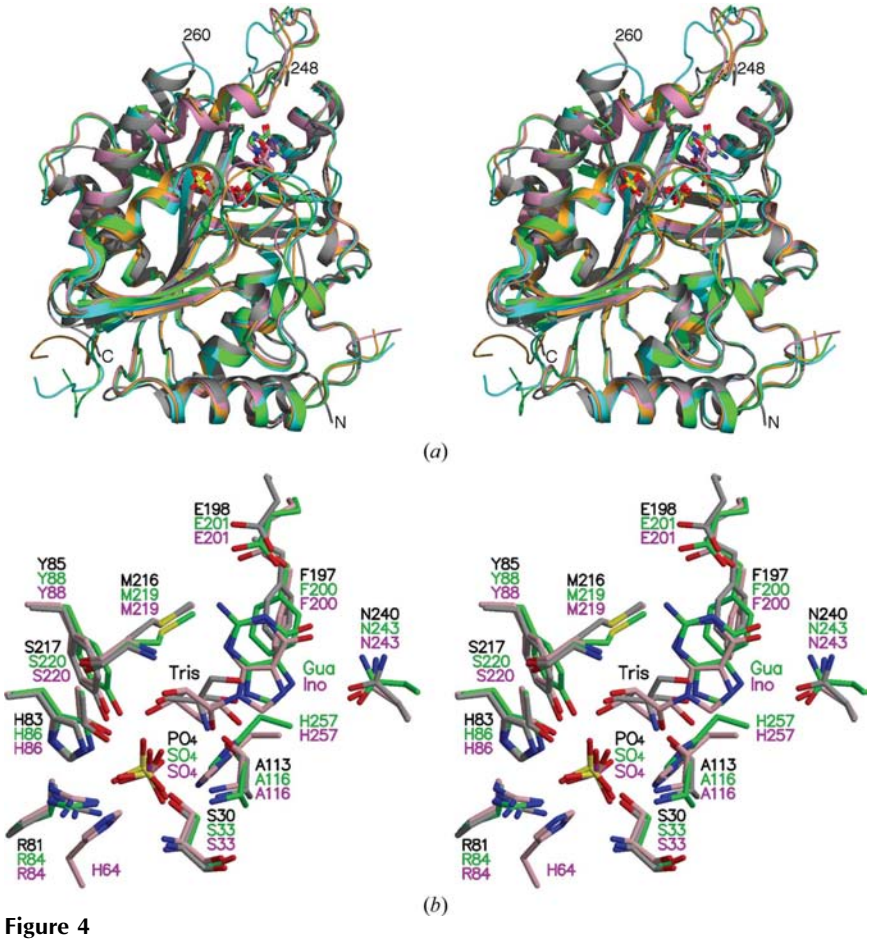

Figure 4
(*a*) Superposition of givPNP–PO_4–Tris (grey) with human PNP–SO_4 (PDB code 1ula, cyan), human PNP–SO_4–guanine (PDB code 1ulb, green), bovine PNP–PO_4 (PDB code 1a9o, orange) and bovine PNP–SO_4–inosine (PDB code 1a9s, pink). The flexible loops in each structure adopt different conformations depending on the ligand binding. (*b*) Active-site superposition of givPNP–PO_4–Tris (grey) with human PNP–SO_4–guanine (PDB code 1ulb, green) and bovine PNP–SO_4–inosine (PDB code 1a9s, pink) complexes in stereo. The atom color codes are the same as in Fig. 2. The catalytically important residues Glu198 and Asn240 of three structures superimpose well.

human PNP–SO_4–guanine complex (PDB code 1ulb) and the bovine PNP–SO_4–inosine complex (PDB code 1a9s). The phosphate-binding sites of all three structures superimpose very well. His61 of givPNP was not built into the present model owing to a lack of density, but the corresponding residue of the bovine enzyme (His64) undergoes a conformational change associated with phosphate binding and makes additional contacts with the phosphate ion (Fig. 4*b*) The conformational changes in loops 33–36 and 56–69 have been reported in all complexes of bovine PNP (corresponding to residues 30–33 and 53–66 of givPNP, respectively) when the phosphate-binding site is occupied (Mao *et al.*, 1998).

Located adjacent to the phosphate-binding site, the ribose-binding site of mammalian PNPs consists of a hydrophobic face containing Tyr88, Met219, Phe200, His257 and Phe159′ around the ribose moiety (numbering is given for human PNP and bovine PNP; subtract three from these numbers for givPNP; Ealick *et al.*, 1990). All of the strictly conserved residues in the ribose-binding site superimpose well between givPNP and other mammalian structures, with the exception of His257. The corresponding His254 in givPNP is disordered and was not included in the final model. In human PNP His257 is important for nucleoside binding by providing a hydrogen bond to the 5′-OH of the ribose ring. Although binding of the Tris molecule in the givPNP structure mimics the ribose binding in the human and bovine structures, a hydrogen-bond interaction with His254 is lacking and probably contributes to the disorder. This observation suggests that His254 in givPNP, like His257 in human PNP, undergoes conformational changes upon substrate binding and might play a role in triggering the active-site flap closure in the presence of the proper substrate.

It has been proposed that the 6-oxopurine specificity of human PNP can be attributed to Asn243 at the active site, which stabilizes the transition state by hydrogen bonding to the purine N7 atom. In contrast, an aspartic acid at the corresponding position in the *E. coli* enzyme is responsible for its broader substrate specificity, acting as a proton donor to N7 of both 6-aminopurine and 6-oxopurines. Protonation stabilizes the negative charge generated from the weakening of the glycosidic bond (Erion, Stoeckler *et al.*, 1997; Mao *et al.*, 1997, 1998). An alternative mechanism has also been proposed for *Cellulomonas* PNP, in which Glu201 plays a role in stabilizing the transition state by accepting a hydrogen bond from N1 of the base, an interaction that is not observed in hexameric PNPs (Tebbe *et al.*, 1999; Bennett *et al.*, 2003; Mao *et al.*, 1997). The equivalent residues in givPNP are Glu198 and Asn240.

Ting and coworkers have reported adenosine phosphorylase activity for givPNP and suggested that the replacement of Lys244 by a valine residue (Val241 in givPNP) might be the reason for this peculiar activity (Ting *et al.*, 2004). The givPNP structural results are inconsistent with this hypothesis. Val241 in the givPNP structure does not appear to be involved in the substrate-binding site. In the published human PNP structure at 2.75 Å resolution, the Lys244 residue pointed away from the active site and was not involved in purine base binding. This observation is consistent with a mutation of Lys244 showing comparable activity to that of wild-type human PNP (Erion, Takabayashi *et al.*, 1997). The amino-acid residue composition and geometrical arrangement in the putative base-binding site suggest that givPNP has a similar substrate specificity to its mammalian orthologs, which has now been confirmed by activity assays with the highly purified enzyme (Table 3).

3.7. givPNP: the unexpected finding of a PNP gene in a virus

The discovery of givPNP is curious because in general viruses do not rely on the purine-salvage pathway, in which degraded nucleic acids are recycled to create a pool of nucleobases. In addition, complete genomic sequence analyses have revealed that the PNP gene is only found in grouper iridovirus and not in any other virus genomes, including other iridoviruses. A similar case has been reported for a double-stranded DNA virus, *Acanthamoeba polyphaga* mimivirus, which encodes genes that are not found in other viruses, such as protein-translation components, proteins implicated in DNA repair and protein folding and proteins involved in new metabolic pathways (Raoult *et al.*, 2004). Of these, preliminary crystallographic analyses of the tyrosyl tRNA synthetase (TyrRS; Abergel *et al.*, 2005) and nucleoside diphosphate kinase (NDK; Jeudy *et al.*, 2005) have been initiated in order to understand their roles in the virus physiology.

Tsai and coworkers suggested that giv has acquired new genes from its host cell, in the case of PNP, or from other co-infecting viruses through gene recombination. In addition, gene recombination is probably responsible for the existence of other unique genes in giv such as a Bcl-2-like gene and host-immunity interfering genes and also the absence of several conserved genes in *Ranavirus* such as DNA methyltransferase, thymidylate synthase and proliferating cell nuclear antigen (Tsai *et al.*, 2005). In general, their short generation times and the large numbers of replicates cause viruses to evolve much faster than any other living organisms (Shackelton & Holmes, 2004). However, it is still unclear whether givPNP is just a fortuitous gene transfer from the host cell or whether it has an essential role in the generation of purine for viral replication.

This work was supported in part by NIH grant CA-67763 to SEE. We thank Leslie Kinsland for assistance in the preparation of this manuscript.

References

Abergel, C., Chenivesse, S., Byrne, D., Suhre, K., Arondel, V. & Claverie, J.-M. (2005). *Acta Cryst.* F**61**, 212–215.
Appleby, T. C., Mathews, I. I., Porcelli, M., Cacciapuoti, G. & Ealick, S. E. (2001). *J. Biol. Chem.* **276**, 39232–39242.
Bennett, E. M., Li, C., Allan, P. W., Parker, W. B. & Ealick, S. E. (2003). *J. Biol. Chem.* **278**, 47110–47118.
Brünger, A. T., Adams, P. D., Clore, G. M., DeLano, W. L., Gros, P., Grosse-Kunstleve, R. W., Jiang, J.-S., Kuszewski, J., Nilges, M., Pannu, N. S., Read, R. J., Rice, L. M., Simonson, T. & Warren, G. L. (1998). *Acta Cryst.* D**54**, 905–921.
Bzowska, A., Kulikowska, E. & Shugar, D. (1990). *Z. Naturforsch. C*, **45**, 59–70.
Bzowska, A., Kulikowska, E. & Shugar, D. (2000). *Pharmacol. Ther.* **88**, 349–425.

Daddona, P. E., Wiesmann, W. P., Milhouse, W., Chern, J. W., Townsend, L. B., Hershfield, M. S. & Webster, H. K. (1986). *J. Biol. Chem.* **261**, 11667–11673.
DeLano, W. L. (2002). *The PyMOL Molecular Graphics System.* DeLano Scientific, San Carlos, California, USA.
Ealick, S. E., Babu, Y. S., Bugg, C. E., Erion, M. D., Guida, W. C., Montgomery, J. A. & Secrist, J. A. III (1991). *Proc. Natl Acad. Sci. USA*, **88**, 11540–11544.
Ealick, S. E., Rule, S. A., Carter, D. C., Greenhough, T. J., Babu, Y. S., Cook, W. J., Habash, J., Helliwell, J. R., Stoeckler, J. D. & Bugg, C. E. (1990). *J. Biol. Chem.* **265**, 1812–1820.
Emsley, P. & Cowtan, K. (2004). *Acta Cryst.* D**60**, 2126–2132.
Erion, M. D., Stoeckler, J. D., Guida, W. C., Walter, R. L. & Ealick, S. E. (1997). *Biochemistry*, **36**, 11735–11748.
Erion, M. D., Takabayashi, K., Smith, H. B., Kessi, J., Wagner, S., Honger, S., Shames, S. L. & Ealick, S. E. (1997). *Biochemistry*, **36**, 11725–11734.
Esnouf, R. (1997). *J. Mol. Graph.* **15**, 132–134.
Gouet, P., Courcelle, E., Stuart, D. I. & Métoz, F. (1999). *Bioinformatics*, **15**, 305–308.
Hammer-Jespersen, K., Buxton, R. S. & Hansen, T. D. (1980). *Mol. Gen. Genet.* **179**, 341–348.
Jakob, N. J., Muller, K., Bahr, U. & Darai, G. (2001). *Virology*, **286**, 182–196.
Jensen, K. F. (1978). *Biochim. Biophys. Acta*, **525**, 346–356.
Jeudy, S., Coutard, B., Lebrun, R. & Abergel, C. (2005). *Acta Cryst.* F**61**, 569–572.
Jones, T. A., Zou, J.-Y., Cowan, S. W. & Kjeldgaard, M. (1991). *Acta Cryst.* A**47**, 110–119.
Kraulis, P. J. (1991). *J. Appl. Cryst.* **24**, 946–950.
Lai, Y. S., Murali, S., Ju, H. Y., Wu, M. F., Guo, I. C., Chen, S. C., Fang, K. & Chang, C. Y. (2000). *J. Fish Dis.* **23**, 379–388.
Laskowski, R. A., MacArthur, M. W., Moss, D. S. & Thornton, J. M. (1993). *J. Appl. Cryst.* **26**, 283–291.
Mao, C., Cook, W. J., Zhou, M., Federov, A. A., Almo, S. C. & Ealick, S. E. (1998). *Biochemistry*, **37**, 7135–7146.
Mao, C., Cook, W. J., Zhou, M., Koszalka, G. W., Krenitsky, T. A. & Ealick, S. E. (1997). *Structure*, **5**, 1373–1383.
Matthews, B. W. (1968). *J. Mol. Biol.* **33**, 491–497.
Merritt, E. A. & Bacon, D. J. (1997). *Methods Enzymol.* **277**, 505–524.
Montgomery, J. A. (1993). *Med. Res. Rev.* **13**, 209–228.
Narayana, S. V. L., Bugg, C. E. & Ealick, S. E. (1997). *Acta Cryst.* D**53**, 131–142.
Otwinowski, Z. & Minor, W. (1997). *Methods Enzymol.* **276**, 307–326.
Parks, R. E. Jr & Agarwal, R. P. (1973). *The Enzymes*, 3rd ed., edited by P. D. Boyer, Vol. 8, pp. 307–334. New York: Academic Press.
Ramachandran, G. N., Ramakrishnan, C. & Sasisekharan, V. (1963). *J. Mol. Biol.* **7**, 95–99.
Raoult, D., Audic, S., Robert, C., Abergel, C., Renesto, P., Ogata, H., La Scola, B., Suzan, M. & Claverie, J. M. (2004). *Science*, **306**, 1344–1350.
Schnitzler, P., Soltau, J. B., Fischer, M., Reisner, H., Scholz, J., Delius, H. & Darai, G. (1987). *Virology*, **160**, 66–74.
Senesi, S., Falcone, G., Mura, U., Sgarrella, F. & Ipata, P. L. (1976). *FEBS Lett.* **64**, 353–357.
Sgarrella, F., Frassetto, L., Allegrini, S., Camici, M., Carta, M. C., Fadda, P., Tozzi, M. G. & Ipata, P. L. (2007). *Biochim. Biophys. Acta*, **1770**, 1498–1505.
Shackelton, L. A. & Holmes, E. C. (2004). *Trends Microbiol.* **12**, 458–465.
Stoeckler, J. D. (1984). *Developments in Cancer Chemotherapy*, edited by R. I. Glazer, pp. 35–60. Boca Raton: CRC Press.
Tebbe, J., Bzowska, A., Wielgus-Kutrowska, B., Schroder, W., Kazimierczuk, Z., Shugar, D., Saenger, W. & Koellner, G. (1999). *J. Mol. Biol.* **294**, 1239–1255.
Thompson, J. D., Gibson, T. J., Plewniak, F., Jeanmougin, F. & Higgins, D. G. (1997). *Nucleic Acids Res.* **24**, 4876–4882.
Ting, J. W., Wu, M. F., Tsai, C. T., Lin, C. C., Guo, I. C. & Chang, C. Y. (2004). *J. Gen. Virol.* **85**, 2883–2892.
Tsai, C. T., Ting, J. W., Wu, M. H., Wu, M. F., Guo, I. C. & Chang, C. Y. (2005). *J. Virol.* **79**, 2010–2023.